ELSEVIER

Contents lists available at ScienceDirect

NanoImpact

journal homepage: www.elsevier.com/locate/nanoimpact





Use of the dustiness index in combination with the handling energy factor for exposure modelling of nanomaterials

Carla Ribalta ^{a,b,*}, Alexander C.Ø. Jensen ^a, Neeraj Shandilya ^c, Camilla Delpivo ^d, Keld A. Jensen ^a, Ana Sofia Fonseca ^a

- ^a The National Research Center for Work Environment (NRCWE), Lersø Parkallé 105, 2100, Copenhagen, Denmark
- ^b Federal Institute for Occupational Safety and Health (BAuA), 10317 Berlin, Germany
- ^c TNO. Princetonlaan 6. 3584 CB Utrecht. Netherlands
- d LEITAT Technological Centre, C/ de Pallars, 179 185, 08005 Barcelona, Spain

ARTICLE INFO

Editor: Bernd Nowack

Keywords: Mass-balance modelling Workplace exposure assessment Emission source Handling energy factor Indoor airflows

ABSTRACT

The use of modelling tools in the occupational hygiene community has increased in the last years to comply with the different existing regulations. However, limitations still exist mainly due to the difficulty to obtain certain key parameters such as the emission rate, which in the case of powder handling can be estimated using the dustiness index (DI). The goal of this work is to explore the applicability and usability of the DI for emission source characterization and occupational exposure prediction to particles during nanomaterial powder handling. Modelling of occupational exposure concentrations of 13 case scenarios was performed using a two-box model as well as three nano-specific tools (Stoffenmanager nano, NanoSafer and GUIDEnano). The improvement of modelling performance by using a derived handling energy factor (H) was explored. Results show the usability of the DI for emission source characterization and respirable mass exposure modelling of powder handling scenarios of nanomaterials. A clear improvement in modelling outcome was obtained when using derived quartile-3 H factors with, 1) Pearson correlations of 0.88 vs. 0.52 (not using H), and 2) ratio of modelled/measured concentrations ranging from 0.9 to 10 in 75% cases vs. 16.7% of the cases when not using H. Particle number concentrations were generally underpredicted. Using the most conservative H values, predictions with ratios modelled/measured concentrations of 0.4–3.6 were obtained.

1. Introduction

Substances produced or imported in quantities over 10 t a year and/ or classified as hazardous according to the CLP regulation EC 1272/2008, require quantitative occupational exposure assessments to comply with the REACH (Registration, Evaluation, Authorization and Restriction of Chemicals) regulation (EC 1907/2006) as amended in the (EU) 2018/1881 regulation. To comply with this, as defined in the ECHA (European Chemical Agency) Guidance R.14 (ECHA R.14, 2016), the occupational exposure assessment may be done using different modelling approaches. The use of models is also included and recommended in the European Standard (EN 689, 2020). This has led to their increasing

use in the occupational hygiene community and in the last years, efforts have been made in order to develop, refine and assess models and tools to support exposure- and overall risk assessment (Cherrie et al., 2020; Dols et al., 2018; Liguori et al., 2016; OECD ENV/CBC/MONO (2021)28, 2021; Schlüter et al., 2022; Spinazzè et al., 2019; Tielemans et al., 2007). Some of the most widely used tools, mentioned in ECHA guidance documents and accepted for use under the REACH regulation for general chemicals, are for example Stoffenmanager¹ ART² or ECETOC TRA.³ However, these tools were not designed and were found not suitable (OECD ENV/CBC/MONO(2021)28, 2021) for assessment of exposure to nanomaterials. Therefore, for nanomaterial assessment, specific tools have been developed in the last years (Dols et al., 2018;

E-mail addresses: ribaltacarrasco.carla@baua.bund.de (C. Ribalta), neeraj.shandilya@tno.nl (N. Shandilya), cdelpivo@leitat.org (C. Delpivo), kaj@nfa.dk (K.A. Jensen), agf@nfa.dk (A.S. Fonseca).

https://doi.org/10.1016/j.impact.2024.100493

 $^{^{\}ast}$ Corresponding author.

https://stoffenmanager.com/

² https://www.advancedreachtool.com/

³ https://www.ecetoc.org/tools/tra-main/

Van Duuren-Stuurman et al., 2012), but most of them (e.g., Stoffenmanager nano, ⁴ NanoSafer⁵ or GUIDEnano⁶) are still under refinement and are not suggested in e.g., ECHA guidances. Aside from the aforementioned models, the use of mass-balance models tailored for specific scenarios has been proposed and studied for worker exposure assessment by several authors in occupational environments (Arnold et al., 2017a; Koivisto et al., 2021, 2015; Ribalta et al., 2021).

However, the use of exposure assessment models and tools by the general occupational hygiene community is currently still limited. This is due to mainly difficulties in determining key parameters needed, such as the emission source strength, which mostly requires chemical principles or measurements to be determined (Schlüter et al., 2022). In this regard, the dustiness index (DI), which is defined as a measure of a material's tendency to generate airborne dust during mechanical or aerodynamic stimulus (Lidén, 2006), has been identified as a useful parameter to characterize the emission source for further modelling of powder handling scenarios (Schneider and Jensen, 2009; Levin et al., 2014; Koivisto et al., 2015; Fonseca et al., 2018; Ribalta et al., 2019a). Some exposure assessment tools such as GUIDEnano or NanoSafer are based on mass-balance models and use the DI as input for emissions source characterization. The DI of powders containing nano-objects, can be relatively easily determined following the existent standardized methodologies (EN 17199:, 2019) which include modifications of the two EN 15051:, 2013 dustiness tests (the rotating drum (RD) and continuous drop (CD)) as well as the small rotating drum (SRD) and the vortex shaker. In addition, due to the special characteristics of high aspect ratio materials and nanomaterials (HARN), the fluidizer method has been developed to achieve disentanglement of agglomerates in individual fibres (Broßell et al., 2019). Each dustiness method is different and intended to simulate different processes, therefore providing considerable different dustiness values. Even though the DI of (nano) materials has been identified as a useful parameter for emission source characterization, further understanding between the link of the different existing dustiness methods and particles emission during specific scenarios is needed (Cherrie et al., 2020). Recent efforts were conducted in order to systematically determine the so-called handling energy factor (H), for pouring or dropping processes for the CD and the SRD dustiness methods (Fonseca et al., n.d., under revision). The H factor is used to adjust the method-specific DI to the process scenario by linking the effective mechanical energy applied during a specific process with the energy used during the dustiness test (Schneider and Jensen, 2007; Fonseca et al., n.d., under revision). Another key parameter with associated uncertainty is the air exchange between the different compartments due to indoor airflows (interzonal airflow; β), which is crucial to estimate how emitted particles move between compartments. The determination of indoor airflows can sometimes be difficult due to complex interactions between room air currents, ventilation systems or temperature (Ganser and Hewett, 2017) as well as contributions from activities and moving parts. Therefore, in many cases airflows will need to be assumed from literature or dispersion tests. Some authors have tried to determine and quantify air changes between compartments (Keil and Zhao, 2017), but a complete understanding it is not yet achieved and discrepancies have been encountered between different techniques (e.g., speed velocities or tracer gas) (Boelter et al., 2009).

The aim of this work is to explore the applicability and usability of the DI for source strength characterization and occupational exposure prediction to particles during mechanical handling of nanomaterial powders, by using the H factors derived in Fonseca et al., n.d. (under revision). The characterized emission source term is later applied as input parameter in a two-box model (Ganser and Hewett, 2017) to calculate estimated exposure concentrations, which are compared to

measured exposure concentrations. The applicability of the DI for exposure prediction is assessed for mass and particle number concentrations and uncertainty due to the different parameters is investigated. Moreover, three nano-specific tools that use DI to determine exposure are tested.

2. Materials and methods

2.1. Case studies

A total of 13 exposure scenarios (cases) from 6 different studies dealing with exposure to nanoparticles during handling of powdered materials were compiled. The cases are described in Table 1.

2.2. Mass-balance modelling

Exposure modelling was performed by using a two-box model (or near-field (NF)/far-field (FF) model) (Ganser and Hewett, 2017) assuming that 1) particles are fully mixed at all times; 2) airborne particles are generated by a source inside the limits of the NF; and 3) particle losses are only due to natural and mechanical ventilations. The model was used to calculate the respirable mass and particle number concentration. Particle losses by sedimentation and coagulation were not considered.

In the two-box model, the mass balance concentration inside the model volume (NF and FF volume) is described as a function of time (Ganser and Hewett, 2017):

- Mass balance in the NF:

$$V_{NF} \frac{dC_{NF}}{d_{t}} = S + \beta \cdot C_{FF} - \beta \cdot C_{NF}$$
 (1)

- Mass balance in the FF:

$$V_{FF} \frac{dC_{FF}}{d_{I}} = \mathbf{Q} \cdot C_{0} + \beta \cdot \mathbf{C}_{NF} - (\beta + \mathbf{Q}) \cdot \mathbf{C}_{FF}$$
 (2)

$$Q = ACH \cdot (V_{NF} + V_{FF}) \tag{3}$$

where

S (mg/min or #/min) is the emission source rate located in the NF; C_0 (mg/m³ or #/cm³) is the concentration entering the FF volume with the incoming air flow (Q), considered 0 in this case;

 C_{NF} and C_{FF} (mg/m³ or #/cm³) are NF and FF concentrations;

 V_{NF} and V_{FF} (m³) are the NF and FF volumes;

Q (m³/min) is the general air flow;

 β (m³/min) is the airflow between NF and FF zones.

Total volumes were reported for all considered cases, and NF volume was assumed to be 8 m³, as a reasonable default value (Cherrie and Schneider, 1999; Ganser and Hewett, 2017) (Table 2).

2.3. Emission source characterization

The emission (S) from the process is described based on the DI (Koivisto et al., 2015):

$$S(t) = DI \bullet H \bullet \frac{dM(t)}{dt} \bullet LC_n$$
 (4)

where

DI (mg/kg or #/kg) is the dustiness index of the material;

H(-) is the handling energy factor for the process;

dM/dt (kg/min) is the mass flow of the material in the process;

 LC_n (–) are the reduction factors of the different local controls in place.

⁴ https://nano.stoffenmanager.com/

⁵ http://www.nanosafer.org/

⁶ https://tool.guidenano.eu/

Table 1

Exposure case number, reference, description, and primary particle size and shape. LEV: local exhaust ventilation, HNT: halloysite nanotubes, MWCNT: multi-walled carbon panotubes.

Case n°	Reference	Description of activity and scenario	Local Controls (LC)	Primary product	Primary object size (nm)	Primary object shape
A1	Koivisto et al. (2015)	Powder handling – Pouring: of 500 kg TiO ₂ (93%) into a discharge cone with rim extraction	Discharge cone with rim extraction	Pigment grade TiO ₂	220*	Spherical /Isometric
A2		Powder handling – Pouring: of 500 kg TiO ₂ (94%) into a discharge cone with rim extraction	Discharge cone with rim extraction	Pigment grade TiO ₂	240*	Spherical /Isometric
A3		Powder handling – Pouring: of 25 kg RD3 TiO ₂ (93%) into a mixer without ventilation	Mixer – Low level containment	Pigment grade TiO ₂	220*	Spherical /Isometric
B1	Fonseca et al. (2021)	Powder handling – Pouring: of 2150 kg of TiO ₂ powder from 86 small bags for paint formulation into a mixer with LEV under the pouring point	Mixer – Low level containment and LEV system	Pigment grade TiO ₂	200*	Spherical /Isometric
B2		Powder handling – Pouring: of 1475 kg of TiO ₂ powder from 59 small bags for paint formulation into a mixer with LEV under the pouring point	Mixer – Low level containment and LEV system	Pigment grade ${ m TiO}_2$	200*	Spherical /Isometric
В3		Powder handling – Pouring: of 2625 kg of TiO ₂ powder from 105 small bags for paint formulation into a mixer with LEV under the pouring point	Mixer – Low level containment and LEV system	Pigment grade ${ m TiO_2}$	200	Spherical /Isometric
C1	H2020 CaLIBRAte project (original data from	Powder handling – Transferring of: SiO ₂ aerogel beads under fume hood	Fume hood	SiO ₂	N/A	Spherical /Isometric
C2	authors; not published) ^a	Handling: Quality tests (handling panels)	No LC	SiO_2	N/A	Spherical /Isometric
D1	Koivisto et al. (2014)	Powder handling – Handling: of Nanodiamonds in a glove box and sieving in a fume chamber	Glove box and fume hood	Nanodiamond	Crystallite size: 4–6**	Rod-shaped/ Spherical
D2		Powder handling – Handling: of Nanodiamonds in an under pressurized glove box and sieving in a room	Glove box	Nanodiamond	Crystallite size: 4–6**	Rod-shaped/ Spherical
E1	Koivisto et al. (2018)	Powder handling – Pouring: of 10 times 100 g of dried HNTs from the trays. A total of 936 g HNTs was poured from ca. 20 cm height into a 6.7 L stainless steel mixing bowl	Fume hood	HNTs	Diameter: 15–45*	Fibre-like
E2		Powder handling – Mixing: of 936 g HNTs with same amount of carvacrol oil in a mixer with a K-beater mixing tip under a fume hood. Mixer covered with splashguard	Fume hood	HNTs	Diameter: 15–45*	Fibre-like
F1	Meyer-Plath et al. (2020) ^b	Powder handling – Handling: of MWCNT in a closed system inside a safety workbench	Safety workbench	MWCNT	Diameter 10–20*	Fibre-like

Determined using electron microscopy methods.

Table 2 Input parameters used for modelling. FZ: fluidizer dustiness method; N/A: not available. *DI is under the detection limit of 7 mg/kg, for modelling purposes, 7 mg/kg was used. * 1 : 133 min of handling in a glove box (LC_n of 0.0001) and 10 min of sieving under fume hood (LC_n of 0.08). * 2 : 107 min of handling in a glove box (LC_n of 0.0001) and 10 min of sieving in a room (LC_n of 1 = no local controls applied).

Case n°	DI _M (mg/kg)	$\mathrm{DI_{N}}$ (#/mg)	H level (–)	dM/dt (kg/min)	$LC_n(-)$	V (m ³)	ACH (1/h)	β (m ³ /min)
A1	SRD: <7 (5.3)*	SRD:160	Н6	33.3	0.25	1500	5	13
A2	SRD: <7 (1.6)*	SRD: 60	Н6	125.0	0.25	1500	5	13
A3	SRD: <7 (5.3)*	SRD:160	Н6	26.0	0.40	1500	5	13
B1	CD: 73.1 SRD: <7 (6.3)*	CD: 5568 SRD: 2460	Н6	39.1	0.40 and 0.36	3010	2	15
B2	CD: 73.1 SRD: <7 (6.3)*	CD: 5568 SRD: 2460	Н6	61.5	0.40 and 0.36	3010	2	15
В3	CD: 73.1 SRD: <7 (6.3)*	CD: 5568 SRD: 2460	Н6	62.5	0.40 and 0.36	3010	2	15
C1	SRD: 1693	N/A	H4	0.44	0.08	70.25	2	6.5
C2	SRD: 1693	N/A	H1	0.15	1	109	3	7.5
D1	SRD: 206	N/A	H6	0.014	$0.006*^{1}$	300	2	9.6
D2	SRD: 206	N/A	H6	0.017	$0.09*^{2}$	300	2	9.6
E1	SRD: 35.5	N/A	Н6	0.50	0.08	1230	3	13
E2	SRD: 35.5	N/A	H7	0.052	0.08	1230	3	13
F1	SRD: 12.7 FZ: 0.00174	SRD: 24000	H4	0.0000009	0.30	71	3	6.6

Using LC_n is a simplification in cases where exposure control is managed by exhaust ventilation in which a higher tier modelling would require knowledge on exhaust ventilation rate and capture efficacy of the system. Values used for modelling are detailed in Table 2.

The H factors used were taken from Fonseca et al., n.d., under revision, where H values linking the energy during a dropping process and during the CD and SRD dustiness tests were derived. The H values derived are valid for dropping processes with a free drop air between 1

^{**} Determined using X-ray diffraction peak with.

^a Additional details on the case study are available in caLIBRAe D7.5.

^b Case ID: WP04.

and 100 cm. In this work, the H quartile-3 (H_{Q3}) values were used as a conservative approach as applied in NanoSafer, but the H quartile-1 (H_{Q1}), mean and maximum (H_{max}) values were also tested. In addition, modelling were performed with a H value of 1 (H_{1}) in order to explore its impact of no modification. Values used are detailed in Table 2 and Supplementary Table S1.

The reduction on the emissions due to LC_n applied was assumed based on publically available values from the Exposure Control Efficacy Library ECEL v3.0 (https://diamonds.tno.nl/ - accessed on the 21/09/2021). Values used are detailed in Table 2 and Supplementary Table S2.

2.4. Air exchange: general air changes per hour (ACH) and interzonal air flow (β)

When available, reported air changes per hour (ACH) were used for modelling. This information was available for A1-A3 and D1-D2. However, when ACH information was not available, worst-case scenario of 2 and 3 1/h were assumed for ordinary factory buildings and laboratories, respectively (Table 2). These values were assumed based on the minimum reported values, for a conservative approach, for these type of environments in The Engineering ToolBox (2005). In addition, to determine the error introduced due to ACH a range of typical values reported for occupational environments (Engineering ToolBox, 2005; Arnold et al., 2017a; Keil and Zhao, 2017), were tested (0.3, 0.5, 0.8, 1, 3, 5, 8, 10 and 30 1/h).

Interzonal airflow or NF-FF air exchange (β ; m³/min) was not reported for any of the cases considered. Therefore, β was extrapolated from ACH using eqs. 5 and 6 (Keil and Zhao, 2017).

$$Q_{NF} = Q_{FF} \cdot \frac{V_{NF}}{V_{tot}} + \left(k_0 + k_0 \cdot log\left(\frac{V_{tot}}{38}\right)\right)$$
 (5)

$$\beta = \frac{1}{2} \cdot FSA.s \tag{6}$$

where

 Q_{NF} and Q_{FF} (m³/min) are the air flows in the NF and FF;

 V_{tot} and V_{NF} (m³) are the total and NF volumes;

 $k \text{ (m}^3/\text{min)}$ describes the convective airflow with k_0 set to 10 m³/min in a 38m³ room (Cherrie, 1999; Cherrie et al., 2011);

FSA (m²) is the free surface area of the NF, which was assumed to be a cube without base;

s (m/min) is the wind speed.

To determine the uncertainty introduced due to β a range of values was tested (0.3, 0.5, 0.8, 1, 3, 5, 8, 10 and 15 m³/min) based on typical reported values (Baldwin and Maynard, 1998; Keil and Zhao, 2017) corresponding to wind speds of 0.03, 0.05, 0.08, 0.1, 0.3, 0.5, 0.8, 1 and 1.5 m/min.

2.5. Risk and exposure assessment tools

The dataset (Table 1) was used to test the performance of three nanospecific exposure assessment tools that use DI as input parameter to estimate the source strength and further modelling of exposure concentrations. The three tools selected, Stoffenmanager nano, NanoSafer, and GUIDEnano, are representative of different levels of complexity, and are able to handle nanomaterial exposure due to powder handling.

Stoffenmanager nano module v1.0 (https://nano.stoffenmanager.com/) is a first tier control banding (CB) tool designed for risk management prioritization in nanomaterial exposure scenarios and to assist implementation of control measures to reduce exposure levels in occupational scenarios (Van Duuren-Stuurman et al., 2012). The tool combines the available hazard information of a substance with a qualitative estimate of potential for inhalation exposure based on the conceptual source-to-receptor model described by Schneider et al. (2011) and modifying factors by Marquart et al. (2008) to categorize the risk in 3 control bands (Van Duuren-Stuurman et al., 2012).

NanoSafer v1.1 beta (http://nanosafer.org/) is a CB and risk management tool made to assess the risk level and recommended exposure control associated with production and use of nanomaterials in workplaces. The tool classifies the hazard in 4 bands taking into account morphology of the primary nanomaterial, chemical surface, the OEL for the nearest analogue bulk material, risk phrases for the nearest analogue bulk material, and water solubility, and 5 exposure bands. The exposure assessment follows the conceptual model described by Schneider et al. (2011) and a theoretical nano-specific exposure limit derived from the hazard assessment and the volume-specific surface area of the nanomaterial. The exposure assessment takes into account the DI combined with the activity handling energy and mass handled in each work cycle, the duration of work cycle and ACH among other parameters. The tool exposure band output value can be converted into a quantitative exposure concentration by using nearest analogue OEL value, volume specific surface area, specific surface area and relative density (Liguori, 2016; Liguori et al., 2016; OECD ENV/CBC/MONO(2021)28, 2021).

GUIDEnano v3.0 (https://tool.guidenano.eu/) is a tool intended to assess human and environmental health risks due of nanomaterials along their life cycle. GUIDEnano provides a quantitative output in terms of an exposure concentration and is based on computational exposure models. The tool requires several input parameters. The exposure condition-related parameters include operational time and frequency, room geometry, ACH, ventilation rate, amount of product used, room temperature and pressure, and personal protective equipment used. The nanomaterial-related parameters include composition, DI, OEL, size distribution, mean diameter, size type (e.g., aerodynamic size, primary size), shape, and density.

2.6. Results assessment

Modelled exposure concentration results obtained were assessed from the ratios of modelled/measured concentrations, the absolute difference, as well as mean absolute error (MAE) and root mean squared error (RMSE).

The percentage of cases for which modelled concentrations were lower than the measured concentrations were determined (ratio modelled/measured <0.9) to assess model underestimation. Percentages for ratios between 0.9 and 5 were determined, considered representative of acceptable modelling outcome in this work. In addition, Spearman and Pearson correlations were calculated.

3. Results

A total of 13 occupational exposure case scenarios resulting in potential nanomaterial exposure during powder handling were used in order to test the applicability of dustiness data for emission source and worker exposure characterization. All 13 cases had SRD data available, whereas only three and one had CD and Fluidizer data, respectively (Table 1). Mainly granular/isometric and granular/rod-shaped nanomaterials (10 cases) compose the data set and, only three cases handle fibre-like nanoparticles. The type of scenarios included are mostly pouring (7), mixing (1), transferring (1) and general handling scenarios (4). Average primary particle sizes range from approximately 10 to 240 nm.

For the two-box modelling assessment, NF modelled concentrations were compared to breathing zone (BZ) or NF measured concentrations, depending on availability. FF modelled concentrations were compared to FF measured concentrations.

3.1. Comparison of modelled and measured respirable mass concentrations

Measured respirable mass concentrations range from 0.00024 to 0.6440 mg/m^3 at the BZ or NF (Table 3), and from 0.022 to 0.051 mg/m^3 at the FF (Table 4). Thus, this work is based on a representative and a

Table 3 Modelling results for respirable mass NF concentrations (mg/m³) using H_{Q3} and H_1 , of the corresponding H level (from Supporting Table S1), and ratio modelled/measured concentrations. Arithmetic standard deviation (σ) associated to the different H, ACH and β values tested, and total. Cases B1-B3 with CD DI. Cases A1-A3, C1-C2, D1-D2, E1-E2 and F1 with SRD DI. *Near field measured concentrations. **Breathing zone measured concentrations.

Case n°	Measured respirable mass concentration (mg/m^3)	Modelled respirable mass concentrations (mg/m³)		Ratio Modelled concentration (using H_{Q3})/ Measured concentration	Model standard deviation due to changes in:				
		Using H _{Q3}	Using H ₁		H σ (mg/m ³)	ACH σ (mg/m ³)	$\beta \sigma$ (mg/m ³)	Total σ (mg/ m ³)	
A1	0.0327*	0.4630	3.0685	14.2	0.2152	0.0540	4.64	4.65	
A2	0.3140*	0.5613	3.7194	1.8	0.2609	0.0672	5.51	5.51	
A3	0.1671*	0.3650	2.4186	2.2	0.1696	0.0090	2.00	2.01	
B1	0.6440*	1.9478	28.644	3.0	0.9542	0.0749	18.81	18.83	
B2	0.4080*	2.7588	40.570	6.8	1.3515	0.0443	18.15	18.20	
В3	0.5750*	3.0264	44.505	5.3	1.4826	0.0890	26.23	26.27	
C1	0.0683*	0.5684	14.999	8.3	0.2500	0.0922	0.8303	0.872	
C2	0.0810*	0.2386	62.795	2.9	0.1034	0.0782	0.6417	0.655	
D1	0.00024*	0.0005	0.0031	2.1	0.0002	0.0002	0.0024	0.002	
D2	0.0050*	0.0083	0.0551	1.7	0.0039	0.0027	0.0413	0.042	
E1	0.0568**	0.0133	0.0878	0.2	0.0062	0.0002	0.0429	0.043	
E2	0.0027**	0.0024	0.0105	0.9	0.0012	0.0001	0.0110	0.011	
F1	N/A	$\begin{array}{c} 3.6 \times \\ 10^{-8} \end{array}$	$\begin{array}{c} 9.5 \times \\ 10^{-7} \end{array}$	N/A	$^{1.6~ imes}_{10^{-8}}$	4.5×10^{-8}	$^{1.0\times}_{10^{-8}}$	1.0×10^{-7}	

Table 4 Modelling results for respirable mass FF concentrations (mg/m³) using H_{Q3} and H_1 , and ratio modelled/measured concentrations. Arithmetic standard deviation (σ) associated to the different H, ACH and β values tested, and total. Cases B1-B3 with CD DI.

Case n°	Measured respirable mass concentration (mg/m^3)	Modelled respirable mass concentrations (mg/m³)		Ratio Modelled concentration (using H_{Q3})/ Measured concentration	Model standard deviation due to changes in:			
		Using H _{Q3}	Using H ₁		H σ (mg/ m ³)	ACH σ (mg/ m ³)	β σ (mg/ m ³)	Total σ (mg/ m ³)
B1	0.0510	0.1485	2.1834	2.9	0.0727	0.0764	0.0269	0.1089
B2	0.0350	0.1317	1.9368	3.7	0.0645	0.0466	0.0369	0.0877
В3	0.0220	0.2014	2.9622	9.0	0.0987	0.0915	0.0434	0.1414

relatively wide range of respirable mass concentrations measured in occupational environments during nanomaterial handling, but without considering very high respirable mass concentrations. Measured respirable mass concentrations were mostly obtained from real-time devices (optical particle counters and electrical low pressure impactor) by converting particle number data to mass. In case E1 and E2, respirable mass concentrations were gravimetrically measured by using a cyclone. Dustiness data used as input for modelling is based on respirable mass concentration gravimetrically measured.

Modelled respirable mass concentrations were calculated by using SRD DI for all cases (Table 3 and Supplementary Table S3), and by using CD DI for cases B1-B3 (Table 3). In Table 3, modelled concentrations are shown for B1-B3 using CD DI (considered to be the method that best resembled the case scenarios) and SRD DI for the rest of the cases.

Modelled respirable mass concentrations using H_{Q3} for granular nanomaterials range from 0.0005 to 3.03 mg/m³ at the NF (Table 3) and from 0.132 to 0.201 mg/m³ at the FF (Table 4). NF modelled concentrations for fibre-like particles range from 3.6 \times 10⁻⁸ to 0.013 mg/m³ using SRD DI (Table 3).

The ratio of NF $\rm H_{Q3}$ modelled/measured concentrations range from 1.7 to 14.2 for granular nanomaterials. Overall, for granular nanomaterials 60% of the cases were predicted within 0.9–5 ratio, and 40% were estimated with ratios between 5 and 15. When the H factor was not included ($\rm H_1$) in the emission source equation, modelled respirable concentrations for granular nanomaterials ranged from 0.0031 to 62.8 mg/m³ (Table 3), with ratios modelled/measured of 11–775 (data not shown). From the 10 cases dealing with granular nanomaterials, 60% were highly overpredicted with ratios >15. Thus, not considering the H factor greatly increased overprediction, and decreased accuracy.

For fibre-like particles, only three cases were available and from these, only two had available respirable mass exposure data. The obtained ratios for modelled/measured concentrations using SRD DI and $\rm H_{Q3}$ were 0.2 and 0.9 for cases E1 and E2, respectively. Conversely, using $\rm H_1$ resulted in ratios modelled/measured of 1.5 and 3.9. For case F1, dustiness data with the fluidizer method was also available and was used for testing. Modelling results without considering the H factor were on the order of 1.3×10^{-10} mg/m³ (data not shown) which is about 1/7000 times the concentrations obtained using the SRD DI. The same difference is observed between the mass-based DI obtained for the two methods (Table 2). It is important to note that the two mass-based DI are determined differently, while for the SRD respirable DI is determined based on gravimetric measurements, it was estimated from online particle number data in the fluidizer method.

A similar behaviour was observed for FF modelled concentrations, with ratios modelled/measured concentrations ranging 2.9–9.0 (Table 4) and 42.8–134.7 (data not shown) for modelled concentrations using H_{Q3} and H_{1} , respectively.

Correlations of modelled and measured respirable mass concentrations for all data set (granular materials and fibres) were explored and are shown in Fig. 1 for NF concentrations, and using data as shown in Table 3. Correlations were performed for $\rm H_{Q3}$ (Fig. 1a) and $\rm H_{1}$ concentrations (Fig. 1b) and in both cases significant positive Spearman correlation coefficients were obtained of 0.881 (H $_{Q3}$) and 0.804 (H $_{1}$) (n12), respectively. However, this was not the case when using Pearson correlation, which was greatly improved when considering H $_{Q3}$ values (r=0.882; R $^2=0.777$; n 12) versus when not considering the H factor (r=0.518; R $^2=0.268$; n 12).

Absolute difference and percentage error between modelled and

C. Ribalta et al. NanoImpact 33 (2024) 100493

NF concentrations using H_{Q3}

Modelled Resp. conc. (mg/m3)

NF concentrations using H₁

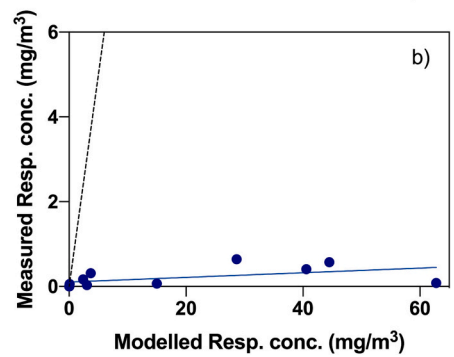


Fig. 1. NF modelled and measured respirable mass concentrations correlation when (a) using the corresponding H_{Q3} value and (b) not considering H factor (H_1) . Solid line shows linear correlation and dashed line indicates line of identity.

measured concentrations is reported in Supplementary Table S4 and S5 for NF and FF concentrations, respectively. The descriptive statistics MAE and RMSE were calculated for H_{Q3} and H_1 and are shown in Table 5. In short, both MAE and RMSE were smaller and closer to 0 when the H_{Q3} factor was considered with values of 1.1×10^{-14} and 3.1 vs. 1.1 and 29.1 for MAE and RMSE, respectively. This indicates a better agreement between modelled and measured values when using the experimental H_{Q3} values than when not considering the H factor (H₁). Therefore, the use of derived H values improves modelling performance but also increase the usability of dustiness data available.

3.2. Uncertainty on modelled respirable mass concentrations due to variations on H, ACH and β

In this work we explored the variability on modelled concentrations due to different possible values for three input parameters, which are sometimes not well known or complex to determine: 1) the H factor, 2) ACH, and 3) NF-FF flows (β). Tested ranges for ACH and β were 0.3, 0.5, 0.8, 1, 3, 5, 8, 10 and 30 1/h, and 0.3, 0.5, 0.8, 1, 3, 5, 8, 10 and 15 m³/min, respectively. For the H factor, H_{Q1}, H_{mean}, H_{Q3} and H_{max} values were tested based on the corresponding H levels from Supplementary Table S1.

Obtained ranges of NF and FF modelled concentrations and corresponding deviation values are shown in Fig. 2, Tables 3 and 4. The lowest variability was introduced by the ACH, with variations between maximum and minimum modelled concentrations of 1–2.5, followed by the H factor, with variations between 3.5 and 4.5. NF modelled concentrations over the tested range of H factor values, and comparison with actual exposures are shown in Fig. 2a for CD and SRD derived modelling results. Overall, the use of the $H_{\rm Q3}$ or even $H_{\rm max}$ values (Fonseca et al., n.d. under revision) is advisable for accurate,

Table 5
Mean absolute error (MAE) and root mean squared error (RMSE) calculated from the difference between NF and FF respirable measured and modelled concentrations. *all cases considered, B1-B3 with CD DI, and all other cases with SRD DI.

Case combination		MAE		RMSE			
		CD SRD A		All cases*	CD	SRD	All cases*
NF	H_{Q3}	2.5	4.2×10^{-18}	1.1×10^{-14}	1.8	0.23	1.1
INI	H_1	16,467.1	$1.7\times\\10^{-3}$	3.1	29.4	18.7	29.1
FF	H_{Q3}	5.6×10^{-4}	$\begin{array}{c} 9.9 \times \\ 10^{-7} \end{array}$	N/A	0.13	0.02	N/A
гг	H_1	4.0	$\begin{array}{c} 2.1 \times \\ 10^{-3} \end{array}$	N/A	2.4	0.20	N/A

precautionary modelling prediction. The use of mean or H_{Q1} values would result in increased modelling underprediction of the exposure concentrations. The parameter introducing the highest error was β , which in turn is the most difficult value to determine and characterize, variations between max and min modelled concentrations of 5.5 to 22.4. However, even though β is the parameter showing higher variability (Fig. 2b), the use of a different β value selected among the ones tested, would only represent a change in terms of whether the modelled concentrations would suffer a change from under to overprediction of measured concentrations or vice versa in three cases (B1, E1 and E2) (Fig. 2b).

3.3. Modelling of particle number concentrations

For the modelling assessment of particle number concentrations only 3 cases (B1-B3) could be used for comparison of NF concentrations. NF background corrected measured particle number concentrations range from 2575 to $5428 \ \#/cm^3$ (Table 6).

The ranges in modelled particle number concentrations using CD DI data are 750.5–1166 $1/\mathrm{cm}^3$, 5952–9248 $\#/\mathrm{cm}^3$ and 2182–3390 $/\mathrm{cm}^3$ when using H_{Q3} , H_{max} , and H_1 respectively (Table 6). Similar modelled particle number concentrations of 748.0–1162 $\#/\mathrm{cm}^3$ were obtained when using SRD DI and H_{Q3} . Conversely, SRD DI modelled concentrations were lower than those obtained with CD DI when using H_1 (964.0–1498 $\#/\mathrm{cm}^3$).

Modelled particle number concentrations using CD and SRD DI for source strength as applied in this work slightly underestimated measured particle number concentrations. Most accurate and precise results were obtained when using CD DI and H_{max} with ratios modelled/measured of 1.1, 1.8 and 3.6. In addition, results show slightly more accurate model performance when using CD DI than SRD. However, additional tests are needed to confirm the results, as limited cases are available.

3.4. Exposure assessment tools

The 13 cases in Table 1 were used to assess the performance of 3 nano-specific exposure assessment tools that use DI as input parameter to calculate the source strength (Stoffenmanager nano, NanoSafer and GUIDEnano). The tools output scores and/or modelled concentrations were compared to measured NF exposure concentrations (Table 7), and Spearman and Pearson coefficient correlations were calculated (Supplementary Fig. S1). For NanoSafer and GUIDEnano, the ratio of modelled/measured concentrations were determined and percentages of modelling underprediction were calculated.

For Stoffenmanager Nano v1.0, the output exposure class score was correlated with measured respirable mass (n11), with Spearman and Pearson correlation coefficients of 0.459 and 0.189. For NanoSafer v1.1

C. Ribalta et al. NanoImpact 33 (2024) 100493

NF H variability

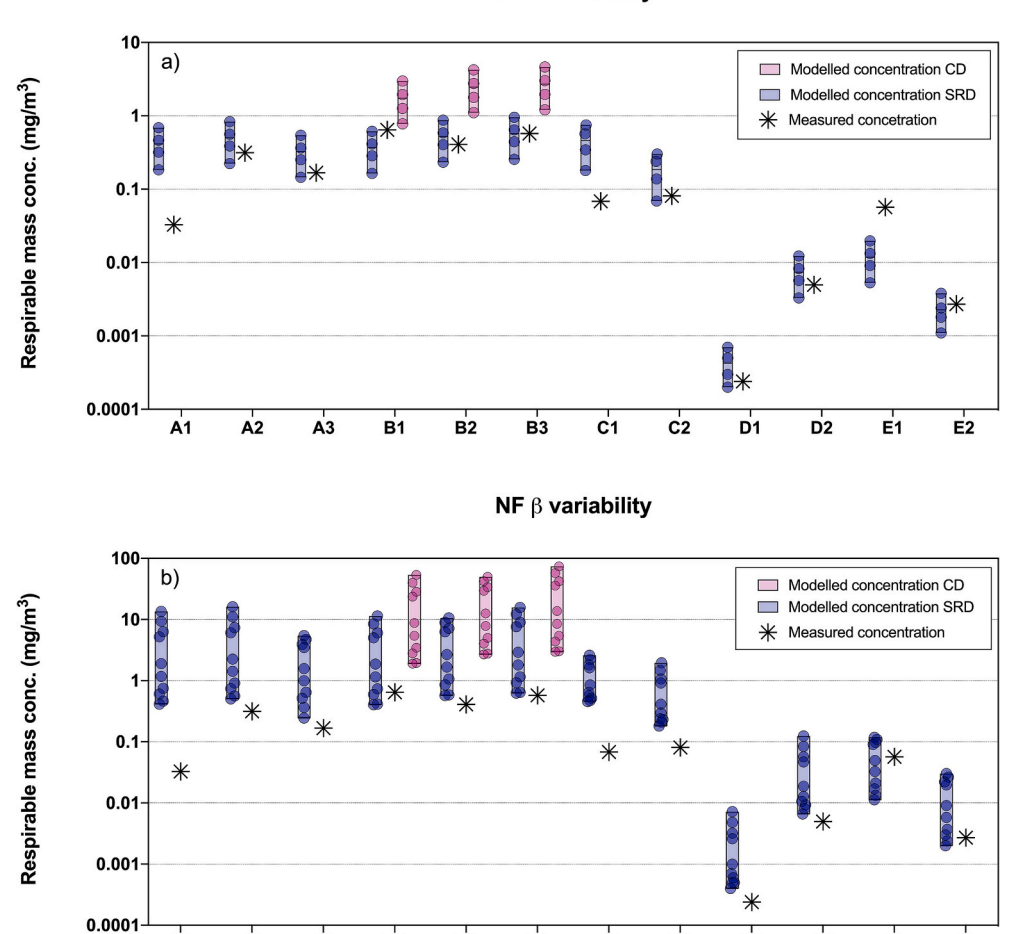


Fig. 2. Range of obtained NF modelled respirable mass concentrations with variations of (a) H and (b) β per case study when using CD and SRD DI. Individual data points represented as filled dots. Solid line indicates H_{03} modelled concentration and β value according Table 2.

В3

C1

D1

מׁח

F1

F2

C2

B₂

Table 6
Modelling results for particle number NF concentrations based on CD DI and SRD (CPC data; total particle number concentration).

B1

DI method	Case n°	DiSCmini Measured (#/cm³)	Modelled (#/cm³)				Ratio Modelled/ Measured					
			H_{Q1}	H_{Mean}	H_{Q3}	H_1	H _{Max}	H_{Q1}	H_{Mean}	H_{Q3}	H_1	H _{Max}
	B1	5428	61.1	1396	750.5	2182	5952	0.011	0.26	0.14	0.40	1.1
CD DI	B2	4793	86.5	1978	1063	3090	8430	0.018	0.41	0.22	0.65	1.8
	В3	2575	94.9	2170	1166	3390	9248	0.037	0.84	0.45	1.3	3.6
	B1	5428	44.7	636	748.0	964.0	2148	0.008	0.12	0.14	0.18	0.40
SRD DI	B2	4793	63.6	901	1060	1365	3042	0.013	0.19	0.22	0.29	0.64
	В3	2575	69.5	989	1162	1498	3337	0.027	0.38	0.45	0.58	1.3

beta, Spearman and Pearson correlation coefficients obtained (n 12) were of 0.552 and 0.731 for NF mass converted from tool output score, and 0.762 and 0.824 for NF mass converted with LC applied. The modelled/measured concentration ratios were calculated for modelled and modelled with LC applied (Table 7) with 25% and 75% of the cases between ratios of 0.9–5, respectively. For GUIDEnano, average mass concentrations show Spearman and Pearson correlations with measured respirable concentrations of 0.750 and 0.353 (n12). The modelled/measured ratios were calculated and it was found that 33.3% of the cases showed ratios between 0.9 and 5.5 whereas 66.7% were lower than 0.9 (0.02–0.76).

A1

A2

Δ3

4. Discussion

Respirable mass concentrations of the total case scenarios (including granular and fibre nanomaterials; n12) were predicted within a ratio range of 0.9–5 with a higher percentage when using derived H_{Q3} values by Fonseca et al., n.d. (under revision) than when using H_1 (58.3% vs. 16.7%). In addition, Pearson and Spearman correlations were improved when using H_{Q3} values compared to not using them. These two facts, plus results from the statistics MEA and RMSE support the idea of the potential usability of the DI to the estimate emission source of a given process and use for exposure modelling, provided that a good linkage between the energy applied during the dustiness test and the process exist (Cherrie et al., 2020; Koivisto et al., 2015; Lidén, 2006; Ribalta et al., 2021; Schneider and Jensen, 2007; Fonseca et al., n.d., under

Table 7

Modelling results of Stoffenmanager nano (exposure class score), NanoSafer (NF score, NF mass converted and NF mass converted with LC applied), and GUIDEnano (average mass concentrations). Cases B1-B3 with CD DI and the rest with SRD DI. *Process is <15 min, acute and peak concentrations used for NanoSafer and GUIDEnano, respectively.

Case	Measured (mg/m³)	NanoSafe	er Original		Stoffen. nano	GUIDEnano			
п°		NF score	NF mass converted	NF mass converted with LC	Ratio modelled/ measured	Ratio modelled LC/measured	Exposure class (time weighted)	Average conc. (mg/m ³)	Ratio modelled long/measured
A1	0.0327	0.029	0.285	0.071	8.7	2.2	2	0.17	3.7
A2	0.3140	0.011	0.108	0.027	0.34	0.09	2	0.19	0.20
A3*	0.1671	0.040*	0.804*	0.322*	4.8*	1.9*	2	0.69*	4.1*
B1	0.6440	0.423	2.39	0.9542	3.7	1.5	2	0.27	0.42
B2	0.4080	0.029	0.166	0.066	0.47	0.16	1	0.17	0.41
В3	0.5750	0.516	2.91	1.165	5.1	2.0	2	0.32	0.56
C1	0.0683	351.6	1.33	0.106	19.4	1.6	2	0.052	0.76
C2	0.0810	21.4	0.081	0.081	1.0	1.0	3	0.45	5.5
D1	0.00024	0.763	0.112	0.0007	466.2	2.9	1	0.000099	0.41
D2	0.0050	0.763	0.112	0.0101	22.4	2.0	1	0.00011	0.02
E1*	0.0568	0.832*	0.755*	0.060*	13.3*	1.1*	N/A	0.0020*	0.04*
E2	0.0027	0.010	0.0015	0.0004	0.56	0.15	1	0.00715	2.7

revision). The ratios obtained for respirable mass concentrations are in line with ratios obtained for non-nano granular powder handling activities (Arnold et al., 2017a; Koivisto et al., 2015; Ribalta et al., 2021, 2019a) as well as general modelling (Arnold et al., 2017b; Jensen et al., 2018; Koivisto et al., 2021; Lopez et al., 2015; Ribalta et al., 2019b). Thus, showing a similar applicability of the methodology for nanomaterials. It is important to note that these results were obtained using a dataset that did not include respirable mass concentrations higher than 0.7 mg/cm³, and the cases were limited in regards to H level representativity, with most cases being around medium H level values. Nine of the cases had a H level of 6, one a H level of 7, two a H level of 4 and one a H level of 1. However, differences on model prediction do not seem to be associated with this fact, for example case C2 (H1 level) shows a ratio modelled/measured concentrations around 3, similar to what is obtained for case B1, with a H6 level.

For fibre-like materials slightly improved modelling performance was obtained when using H_1 . This, could indicate that H values specifically derived for fibre-like nanoparticles are needed. This is plausible considering the behavioural differences between granular and fibre-like aerosols and the fact that H values used were derived using kaolin, clay and talc materials with a plate-like shape (Fonseca et al., n.d. under revision). Overall, the results seem to indicate that the methodology has potential applicability to determine respirable mass concentrations of fibres given the similarity of the ratios obtained with those for granular nanomaterials. However, further research considering the specificities of fibre-like nanoparticles is required.

Effectiveness of the different control measures applied in this work was extracted from the ECEL v3.0 database (as detailed in Supplementary Table S2). A median of the reported values was used and the corresponding multiplying factor was applied to the source term. This is a simplification given that for a higher tier model additional knowledge on the e.g., ventilation rates and collection efficacies are needed. However, it is important to note that the efficacy variability for the different type of risk management measures is known to be substantial and depends on different aspects such as specific settings and characteristics as well as operational and behavioural conducts (Fransman et al., 2008). Given the complexity and data limitation for efficacies, uncertainty on model output due to efficacy controls was not assessed.

For particle number concentrations, only three cases were available with relatively low particle number concentrations when compared to general reported values in literature (Viitanen et al., 2017). Thus, further studies should consider higher number of cases covering a broader range of particle number concentrations. The use of H_{max} showed improved model prediction and accuracy (ratios 1.1–3.6 with CD) when compared to using H_1 (0.4–1.3 with CD). This indicates that 1) modelling particle number concentrations from DI data is possible; 2)

specifically derived H factors are needed; and 3) for an improved performance and precaution, the use of H_{max} is advisable. As opposed to respirable mass concentration, where H_{Q3} or H_{max} were both seen to provide good modelling results, for particle number H_{O3} provided underestimations of the measured particle number concentrations. A possible explanation for this is the difference related to the instrumentation used. Measured particle number concentrations are given by the DiSCmini, whereas DI data used to calculate emission rates as well H derived values were obtained using the CPC 3007. Differences on measured concentrations by these two instruments have been previously described (Mills et al., 2013). Other plausible explanations are 1) lower number of data points used for determining the H factors for particle number than respirable mass concentrations; and 2) behavioural differences between aerosols generated during pouring simulation for H determination with talc, clay and kaolin materials and during the specific modelled cases with the specific nanomaterials.

Although, the results seem favourable to the usability of dustiness for exposure modelling of respirable mass and particle number concentrations, there is still room for improvement for a more robust predicted exposure assessment. In this regard, there are several aspects, which require further research. On the one hand, H factors used were derived 1) using clay, talc and kaolin, with limited material shape representation (isometric and plate-like shapes) and, 2) simulating a drop process by pouring materials into an open bucket, and using free-drop height to link the energy applied. However, in some real exposure cases, pouring occurs into a liquid and moreover usually through a tank or mixer opening. This is expected to have an impact on the released particle number and mass. It is still not known whether the total drop height (total distance of the material fall until the bottom of e.g., mixer) would be a better estimate than the drop height in free air, which currently is used in the H factors determination and use. On the other hand, the dustiness kinetics (e.g., particle generation rate and time required to generate 50% of the particles emitted) seem to have an important role on describing the aerosol dynamics of emitted particles (Schneider and Jensen, 2007; Levin et al., 2014; EN 17199-4:, 2019; Fonseca et al., n.d. under revision). This information can be especially beneficial for example, when modelling repetitive processes, as the number of repetitions can have a higher impact on the concentrations than the time duration or amount of material (Koponen et al., 2015; Ribalta et al., 2019c). Therefore, the improvement and addition of modifying factors to determine the emission source could be key for improving modelling performance and needs further research.

For Stoffenmanager nano, the Spearman correlation coefficient (0.46) differs from the coefficient obtained for particle number concentration in previous work (0.78), which considered a larger dataset (n 82) and broader particle number concentration range (OECD ENV/CBC/

MONO(2021)28, 2021). In the cited work, the tool was observed to have the tendency to overestimate low exposures. For NanoSafer, Spearman and Pearson correlation coefficients and percentage of predicted values within 0.9-5 ratio range are comparable to those obtained using the two-box mass-balance model for this data set and with the specified modelling settings, especially after application of the LC reduction. Moreover, the Spearman correlation found for NanoSafer (0.76) is comparable to the obtained correlation in previous work (0.72) using a larger dataset (n30) (OECD ENV/CBC/MONO(2021)28, 2021). For GUIDEnano Spearman and Pearson correlation coefficients and ratios modelled/measured concentrations are in line with those obtained using the two-box mass-balance model, but slightly lower. The tool was observed to generally underestimate concentrations for the cases used in this dataset and with the specified modelling inputs. These results are of relevance considering ongoing discussions regarding best approaches to estimate worker exposure concentrations (Schlüter et al., 2022).

5. Conclusions

The obtained results demonstrate 1) the usability of the dustiness concept for respirable mass exposure modelling of powder handling scenarios (pouring/transferring) of granular nanomaterials, and 2) the clear improvement of this concept by using a derived handling energy factor (H) based on the following key findings:

- Not considering the H factor resulted in highly overpredicted workplace dust concentrations. Conversely, the use of a derived H factor clearly improved modelling precision and accuracy.
- Overall NF concentrations for granular particles were predicted (applying the H_{Q3} factor) in a ratio range 0.9–10 when using CD DI (n3) and SRD DI (n10) in 100% and 80% of the cases, respectively. From the rest of the cases, one has a ratio slightly over 10, whereas the other has a ratio of 0.64.
- Not only precision and accuracy were improved when using the derived H factor values, but Pearson and Spearman correlations as well, with values of 0.88 and 0.88 when considering H factor vs. 0.80 and 0.52 when not considering it.
- The good prediction of respirable mass concentration is true for both NF and FF respirable mass concentrations, although only 3 cases are available for FF concentrations.
- Only three cases dealing with fibres were included in this work.
 Results are not conclusive, and slight underestimation of measured concentration using SRD DI was observed, but the methodology seems to be applicable to fibre-like nanomaterials.

In addition, from the model variability assessment due to changes on ACH, β and H factor, results suggest that the parameter β introduced the highest variability. However, only the lowest value was found to have a significant change on the model output. Thus, the use of assumed values based on literature can provide acceptable modelling results. Results on the application of the concept of using DI and H factor for modelling particle number concentrations demonstrate a potential applicability of the method, but further work is required to improve modelling performance since slight underprediction of measured concentrations was found on the case studies. From the three nano-specific tools tested, NanoSafer was seen to provide most comparable results to the two-box mass-balance modelling performed. GUIDEnano results were also comparable but measured concentrations were generally underpredicted. Stoffenmanager nano comparability was difficult due to low number of cases and differences in output (exposure category vs. concentration). This shows the potential usability of nano-specific tools for exposure prediction but also highlights the need for 1) further improvements and 2) guidelines on the tool's usability.

Funding

This work was financially supported by Gov4Nano Project, funded by the European Union's Horizon 2020 research and innovation programme under Grant Agreement No 814401, and Danish Government (FFIKA, Focused Research Effort on Chemicals in the Working Environment).

CRediT authorship contribution statement

Carla Ribalta: Writing – review & editing, Writing – original draft, Visualization, Methodology, Investigation, Formal analysis, Data curation, Conceptualization. Alexander C.Ø. Jensen: Writing – review & editing, Methodology, Data curation, Conceptualization. Neeraj Shandilya: Writing – review & editing, Investigation, Formal analysis. Camilla Delpivo: Writing – review & editing, Methodology, Investigation, Formal analysis. Keld A. Jensen: Writing – review & editing, Supervision, Project administration, Investigation, Funding acquisition, Conceptualization. Ana Sofia Fonseca: Writing – review & editing, Writing – original draft, Supervision, Methodology, Investigation, Formal analysis, Data curation, Conceptualization.

Declaration of competing interest

The authors declare the following financial interests/personal relationships which may be considered as potential competing interests:

NanoSafer v1.1beta was developed under lead by NRCWE. K.A.J led the development and implementation and it is the main contact point. A. C. \emptyset .J. was periodically involved in minor web-tool revisions. C.R and A. G.F, affiliated to NRCWE, did not take part in the development of the tool

TNO was involved in the conceptual model development of Stoffenmanager nano. N.S. is currently affiliated to TNO but did not participate in the development of the tool.

GUIDEnano Tool was developed by Leitat. C.D, currently affiliated to Leitat, participated in the development of the tool.

Data availability

Data will be made available on request.

Appendix A. Supplementary data

Supplementary data to this article can be found online at https://doi.org/10.1016/j.impact.2024.100493.

References

- Arnold, Susan F., Shao, Y., Ramachandran, G., 2017a. Evaluation of the well mixed room and near-field far-field models in occupational settings. J. Occup. Environ. Hyg. 14, 694–702. https://doi.org/10.1080/15459624.2017.1321843.
- Arnold, Susan F., Shao, Y., Ramachandran, G., 2017b. Evaluating well-mixed room and near-field–far-field model performance under highly controlled conditions. J. Occup. Environ. Hyg. 14, 427–437. https://doi.org/10.1080/15459624.2017.1285492.
- Baldwin, P.E.J., Maynard, A.D., 1998. A survey of wind speeds in indoor workplaces. Ann. Occup. Hyg. 42, 303–313.
- Boelter, F.W., Simmons, C.E., Berman, L., Scheff, P., 2009. Two-zone model application to breathing zone and area welding fume concentration data. J. Occup. Environ. Hyg. 6, 289–297. https://doi.org/10.1080/15459620902809895.
- Broßell, D., Heunisch, E., Meyer-Plath, A., Bäger, D., Bachmann, V., Kämpf, K., Dziurowitz, N., Thim, C., Wenzlaff, D., Schumann, J., Plitzko, S., 2019. Assessment of nanofibre dustiness by means of vibro-fluidization. Powder Technol. 342, 491–508. https://doi.org/10.1016/j.powtec.2018.10.013.
- Cherrie, J.W., 1999. The effect of room size and general ventilation on the relationship between near and far-field concentrations. Appl. Occup. Environ. Hyg. 14, 539–546. https://doi.org/10.1080/104732299302530.
- Cherrie, J.W., Schneider, T., 1999. Validation of a new method for structured subjective assessment of past concentrations. Ann. Occup. Hyg. 43, 235–245. https://doi.org/ 10.1016/S0003-4878(99)00023-X.
- Cherrie, J.W., MacCalman, L., Fransman, W., Tielemans, E., Tischer, M., Van Tongeren, M., 2011. Revisiting the effect of room size and general ventilation on the

- relationship between near- and far-field air concentrations. Ann. Occup. Hyg. 55, 1006–1015. https://doi.org/10.1093/annhyg/mer092.
- Cherrie, J.W., Fransman, W., Heussen, G.A.H., Koppisch, D., Jensen, K.A., 2020. Exposure models for reach and occupational safety and health regulations. Int. J. Environ. Res. Public Health 17, 383. https://doi.org/10.3390/ijerph17020383.
- Dols, W.S., Persily, A.K., Polidoro, B.J., 2018. Development of CPSC Nano-particle Modeling Tools. Gaithersburg, MD. https://doi.org/10.6028/NIST.TN.2004.
- ECHA, "Guidance on Information Requirements and Chemical Safety Assessment. Chapter R.14: Occupational exposure assessment" Version 3.0 August 2016. [Online]. Available: https://echa.europa.eu/documents/10162/13632/informat ion_requirements_r14_en.pdf/bb14b581-f7ef-4587-a171-17bf4b332378. doi: https://doi.org/10.2823/678250.
- EN 15051, 2013. Workplace Exposure Measurement of the Dustiness of Bulk Materials.
- EN 17199, 2019. Workplace exposure Measurement of Dustiness of Bulk Materials that Contain or Release Respirable NOAA and Other Respirable Particles.
- EN 17199-4, 2019. Workplace Exposure Measurement of Dustiness of BULK Materials that Contain or Release Respirable NOAA and Other Respirable Particles Part 4: Small Rotating Drum Method.
- EN 689, 2020. Workplace Exposure Measurement of Exposure by Inhalation to Chemical Agents - Strategy for Testing Compliance with Occupational Exposure Limit Values.
- Fonseca, A.S., Kuijpers, E., Kling, K.I., Levin, M., Koivisto, A.J., Nielsen, S.H., Koponen, I. K., 2018. Particle release and control of worker exposure during laboratory-scale synthesis, handling and simulated spills of manufactured nanomaterials in fume hoods. J. Nanopart. Res. 20, 1–15.
- Fonseca, A.S., Viitanen, A.-K., Kanerva, T., Säämänen, A., Aguerre-Chariol, O., Fable, S., Dermigny, A., Karoski, N., Fraboulet, I., Koponen, I.K., Delpivo, C., Vilchez Villalba, A., Vázquez-Campos, S., Østerskov Jensen, A.C., Hjortkjær Nielsen, S., Sahlgren, N., Clausen, P.A., Xuan Nguyen Larsen, B., Kofoed-Sørensen, V., Alstrup Jensen, K., Koivisto, J., 2021. Occupational exposure and environmental release: the case study of pouring TiO2 and filler materials for paint production. Int. J. Environ. Res. Public Health 18, 418. https://doi.org/10.3390/ijerph18020418.
- Fonseca, A.S., Ribalta, C., Shandilya, N., Fransman, W., Jensen, K.A. Under revision. Development of handling energy factors for use of dustiness data in exposure assessment modelling. Ann. Work Expo. Health., Accepted 2024.
- Fransman, W., Schinkel, J., Meijster, T., Van Hemmen, J., Tielemans, E., Goede, H., 2008. Development and evaluation of an exposure control efficacy library (ECEL). Ann. Occup. Hyg. 52 (7), 567–575.
- Ganser, G.H., Hewett, P., 2017. Models for nearly every occasion: part II two box models. J. Occup. Environ. Hyg. 14, 58–71. https://doi.org/10.1080/ 15459624.2016.1213393 To.
- Jensen, A., Dal Maso, M., Koivisto, A., Belut, E., Meyer-Plath, A., Van Tongeren, M., Sánchez Jiménez, A., Tuinman, I., Domat, M., Toftum, J., Koponen, I., 2018. Comparison of geometrical layouts for a multi-box aerosol model from a single-chamber dispersion study. Environments 5, 52. https://doi.org/10.3390/ environments5050052.
- Keil, C., Zhao, Y., 2017. Interzonal airflow rates for use in near-field far-field workplace concentration modeling. J. Occup. Environ. Hyg. 14, 793–800. https://doi.org/ 10.1080/15459624.2017.1334903.
- Koivisto, A., Palomäki, J., Viitanen, A.-K., Siivola, K., Koponen, I., Yu, M., Kanerva, T., Norppa, H., Alenius, H., Hussein, T., Savolainen, K., Hämeri, K., 2014. Range-finding risk assessment of inhalation exposure to nanodiamonds in a laboratory environment. Int. J. Environ. Res. Public Health 11, 5382–5402. https://doi.org/10.3390/jierph110505382.
- Koivisto, A.J., Jensen, A.C.Ø., Levin, M., Kling, K.I., Maso, M.D., Nielsen, S.H., Jensen, K. A., Koponen, I.K., 2015. Testing the near field/far field model performance for prediction of particulate matter emissions in a paint factory. Environ Sci Process Impacts 17, 62–73. https://doi.org/10.1039/C4EM00532E.
- Koivisto, A.J., Bluhme, A.B., Kling, K.I., Fonseca, A.S., Redant, E., Andrade, F., Hougaard, K.S., Krepker, M., Prinz, O.S., Segal, E., Hollânder, A., Jensen, K.A., Vogel, U., Koponen, I.K., 2018. Occupational exposure during handling and loading of halloysite nanotubes – a case study of counting nanofibers. NanoImpact 10, 153–160. https://doi.org/10.1016/j.impact.2018.04.003.
- Koivisto, A.J., Spinazzè, A., Verdonck, F., Borghi, F., Löndahl, J., Koponen, I.K., Verpaele, S., Jayjock, M., Hussein, T., Lopez de Ipiña, J., Arnold, S., Furxhi, I., 2021. Assessment of exposure determinants and exposure levels by using stationary concentration measurements and a probabilistic near-field/far-field exposure model. Open Res. Eur. 1, 72. https://doi.org/10.12688/openreseurope.13752.1.
- Koponen, I.K., Koivisto, A.J., Jensen, K.A., 2015. Worker exposure and high timeresolution analyses of process-related submicrometre particle concentrations at mixing stations in two paint factories. Ann. Occup. Hyg. 59, 749–763. https://doi. org/10.1093/annhyg/mev014.
- Levin, M., Koponen, I.K., Jensen, K.A., 2014. Release and exposure assessment of four pharmaceutical powders based on dustiness and evaluation of damaged HEPA filters. J. Occup. Environ. Hyg. 11 (3), 165–177. https://doi.org/10.1080/ 15459624.2013.848038.

- Lidén, G., 2006. Dustiness testing of materials handled at workplaces. Ann. Occup. Hyg. 50, 437–439. https://doi.org/10.1093/annhyg/mel042.
- Liguori, B., 2016. Occupational Exposure Assessment of Nanomaterials Using Control Banding Tools. Technical University of Denmark, DTU Environment.
- Liguori, B., Hansen, S.F., Baun, A., Jensen, K.A., 2016. Control banding tools for occupational exposure assessment of nanomaterials - ready for use in a regulatory context? NanoImpact 2, 1–17. https://doi.org/10.1016/j.impact.2016.04.002.
- Lopez, R., Lacey, S.E., Jones, R.M., 2015. Application of a two-zone model to estimate medical laser-generated particulate matter exposures. J. Occup. Environ. Hyg. 12, 309–313. https://doi.org/10.1080/15459624.2014.989361.
- Marquart, H., Heussen, H., Le Feber, M., Noy, D., Tielemans, E., Schinkel, J., West, J., Van Der Schaaf, D., 2008. "Stoffenmanager", a web-based control banding tool using an exposure process model. Ann. Occup. Hyg. https://doi.org/10.1093/annhyg/ men032.
- Meyer-Plath, A., Bäger, D., Dziurowitz, N., Perseke, D., Simonow, B.K., Thim, C., Plitzko, S., 2020. A practicable measurement strategy for compliance checking number concentrations of airborne nano-and microscale fibers. Atmosphere 11 (11), 1254
- Mills, J.B., Park, J.H., Peters, T.M., 2013. Comparison of the DiSCmini aerosol monitor to a handheld condensation particle counter and a scanning mobility particle sizer for submicrometer sodium chloride and metal aerosols. J. Occup. Environ. Hyg. 10, 250. https://doi.org/10.1080/15459624.2013.769077.
- OECD ENV/CBC/MONO(2021)28, 2021. Evaluation of Tools and Models for Assessing Occupational and Consumer Exposure to Manufactured Nanomaterials-Part II: Performance testing results of tools/models for occupational exposure Project: Assessing the Global Readiness of Regulatory and Non-regu.
- Ribalta, C., Koivisto, A.J., López-Lilao, A., Estupiñá, S., Minguillón, M.C., Monfort, E., Viana, M., 2019a. Testing the performance of one and two box models as tools for risk assessment of particle exposure during packing of inorganic fertilizer. Sci. Total Environ. 650 https://doi.org/10.1016/j.scitotenv.2018.09.379.
- Ribalta, C., Koivisto, A.J., Salmatonidis, A., López-Lilao, A., Monfort, E., Viana, M., 2019b. Modeling of high nanoparticle exposure in an indoor industrial scenario with a one-box model. Int. J. Environ. Res. Public Health 16. https://doi.org/10.3390/ ijerph16101695.
- Ribalta, C., López-Lilao, A., Estupiñá, S., Fonseca, A.S., Tobías, A., García-Cobos, A., Minguillón, M.C., Monfort, E., Viana, M., 2019c. Health risk assessment from exposure to particles during packing in working environments. Sci. Total Environ. 671, 474–487. https://doi.org/10.1016/j.scitotenv.2019.03.347.
- Ribalta, C., López-Lilao, A., Fonseca, A.S., Jensen, A.C.Ø., Jensen, K.A., Monfort, E., Viana, M., 2021. Evaluation of one- and two-box models as particle exposure prediction tools at industrial scale. Toxics 9. https://doi.org/10.3390/TOXICS9090201. Page 201 9. 201.
- Schlüter, U., Arnold, S., Borghi, F., Cherrie, J., Fransman, W., Heussen, H., Jayjock, M., Jensen, K.A., Koivisto, J., Koppisch, D., Meyer, J., Spinazzè, A., Tanarro, C., Verpaele, S., von Goetz, N., 2022. Theoretical background of occupational-exposure models—Report of an expert workshop of the ISES Europe Working Group "Exposure Models.". Int. J. Environ. Res. Public Health 19, 1234. https://doi.org/10.3390/ijerph19031234.
- Schneider, T., Jensen, K.A., 2007. Combined single-drop and rotating drum dustiness test of fine to Nanosize powders using a small drum. Ann. Occup. Hyg. 52, 23–34. https://doi.org/10.1093/annhyg/mem059.
- Schneider, T., Jensen, K.A., 2009. Relevance of aerosol dynamics and dustiness for personal exposure to manufactured nanoparticles. J. Nanopart. Res. 11, 1637–1650.
- Schneider, T., Brouwer, D.H., Koponen, I.K., Jensen, K.A., Fransman, W., Van Duuren-Stuurman, B., Van Tongeren, M., Tielemans, E., 2011. Conceptual model for assessment of inhalation exposure to manufactured nanoparticles. J. Expo. Sci. Environ. Epidemiol. 21, 450–463. https://doi.org/10.1038/jes.2011.4.
 Spinazzè, Borghi, Campagnolo, Rovelli, Keller, Fanti, Cattaneo, Cavallo, 2019. How to
- Spinazzè, Borghi, Campagnolo, Rovelli, Keller, Fanti, Cattaneo, Cavallo, 2019. How to obtain a reliable estimate of occupational exposure? Review and discussion of models' reliability. Int. J. Environ. Res. Public Health 16, 2764. https://doi.org/ 10.3390/ijerph16152764.
- The Engineering ToolBox, 2005. Air Change Rates in typical Rooms and Buildings [online] Available at: https://www.engineeringtoolbox.com/air-change-rate-room-d.867.html [Accessed 26 October 2023].
- Tielemans, E., Warren, N., Schneider, T., Tischer, M., Ritchie, P., Goede, H.,
 Kromhout, H., Van Hemmen, J., Cherrie, J.W., 2007. Tools for regulatory assessment of occupational exposure: development and challenges. J. Expo. Sci. Environ.
 Epidemiol. 17, S72–S80. https://doi.org/10.1038/sj.jes.7500604.
 Van Duuren-Stuurman, B., Vink, S.R., Verbist, K.J.M., Heussen, H.G.A., Brouwer, D.H.,
- Van Duuren-Stuurman, B., Vink, S.R., Verbist, K.J.M., Heussen, H.G.A., Brouwer, D.H., Kroese, D.E.D., Van Niftrik, M.F.J., Tielemans, E., Fransman, W., 2012.
 Stoffenmanager nano version 1.0: a web-based tool for risk prioritization of airborne manufactured nano objects. Ann. Occup. Hyg. 56, 525–541. https://doi.org/10.1093/ANNHYG/MER113.
- Viitanen, A.K., Uuksulainen, S., Koivisto, A.J., Hämeri, K., Kauppinen, T., 2017. Workplace measurements of ultrafine particles—a literature review. Ann. Work Expo. Health. 61 (7), 749–758.